# Supporting Information

# Effect of thermal treatment temperature of RuNi bimetallic nanocatalyst on its catalytic performance for benzene hydrogenation

Lihua Zhu,[*,a,b] Jinbao Zheng,[b] Changlin Yu,[a] Nuowei Zhang,[b] Qing Shu,[a] Hua Zhou,[b] Yunhua Li,[b] Bing H Chen[*,b]

[a]School of Metallurgy and Chemical Engineering, Jiangxi University of Science and Technology, Ganzhou 341000, Jiang Xi, China

[b]Department of Chemical and Biochemical Engineering, National Engineering Laboratory for Green Productions of Alcohols-Ethers-Esters, College of Chemistry and Chemical Engineering, Xiamen University, Xiamen 361005, China

**Table S1** Catalytic performance of unsupported and supported metal catalysts for benzene hydrogenation to cyclohexane reported in the literatures

| Ref | Catalyst | t (h) | P ($H_2$) (MPa) | T (℃) | TOF ($h^{-1}$) | Yield to cyclohexane |
|---|---|---|---|---|---|---|
| 1 | 2mol%Perfluoro-tagged Ru1 | 0.5 | 0.1 | 60 | 29 | 34% |
| 2 | 4.2wt%Ru/C-silica 2 | 0.53 | 8.0 | 110 | 37700 | 99.8% |
| 3 | 0.27%Ru/NFS [3] | 2.25 | 0.29 | 25 | 5430 | 100% |
| 4 | 3.3wt%Ru/MMT[4] | 2.5 | 8 | 110 | 4000 | 100% |
| 5 | 4.6%Ru/rGO[5] | 1 | 4.0 | 130 | 38000 | 61.3% |
| 6 | Ru/CNTs [6] | 0.5 | 4.0 | 80 | 6983 | 99.97% |
| 7 | 0.1wt%Pd/$SiO_2$[7] | 2 | 0.83 | 140 | 10000 | 14% |
| 8 | Ir NPs@zeolite[8] | 8 | 0.3 | 25 | 3190 | 100% |
| 9 | Rh/HEA-C16[9] | 5 | 0.1 | 20 | 60 | 100% |
| 10 | 11.2wt%Rh/MWNTs[10] | 3 | 1 | 20 | 1038 | 80% |
| 11 | 0.7wt%Rh(cod)-9.86wt%Pd/$SiO_2$[11] | 2 | 3 | 40 | 1241 | 52% |
| 12 | 6.3wt%Pd-6.9wt%Rh/CNT[12] | 24 | 1 | 20 | 592.6 | 100% |
| 13 | $Rh_{0.5}Ni_{0.5}$[13] | 7 | 4.0 | 25 | 290 | 50.8% |
| This work | RuNi/C~680~PVP | 1 | 5.3 | 60 | 5300 | 29.1% |
| This work | RuNi/C~380 | 1 | 5.3 | 60 | 7750 | 42.5% |

As shown in Table S1, the RuNi/C~680~PVP catalyst exhibited relatively high catalytic performance in benzene hydrogenation reaction compared to a number of supported and unsupported Ru-based, Rh-based, Pd-based, Ir-based and bimetallic-based catalysts reported in the literatures.

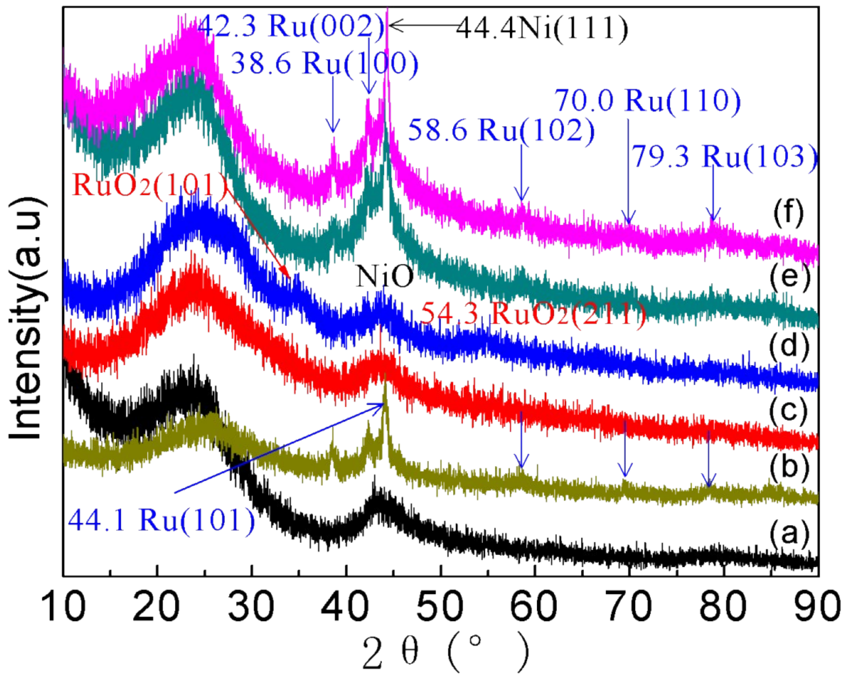


**Fig. S1** XRD patterns for the RuNi/C~X~PVP samples. (a) carbon~380, (b) 2.5%Ru/C~600~$N_2$+$H_2$, (c) RuNi/C~380~PVP, (d) RuNi/C~480~PVP, (e) RuNi/C~580~PVP and (f) RuNi/C~680~PVP. The blue, red and black arrows represent the characteristic diffraction peaks of Ru, $RuO_2$ and Ni crystallite phase, respectively. The two broad peaks at 2θ = 24°, 43° in the XRD patterns are attributed to carbon(002) and (100).[14-16]

Fig. S1a shows the characteristic peaks of hcp Ru (JCPDS card No. 06-0663). For the RuNi/C~X~PVP catalysts, only the diffraction peaks of carbon(002) and carbon(100) can be observed in the XRD patterns when the annealing temperature below or equal to 380 °C, indicating that the Ni, NiO, Ru or RuNi nanoparticles (NPs) were either very small or amorphous, and with high dispersion. When RuNi/C~uncalcined~PVP treated in flowing $N_2$ at 480 °C for 3 h, the NiO(200) (2θ=43.3°) (JCPDS card No. 47-1049), $RuO_2$(101) (2θ=35.0°) and $RuO_2$(211) (2θ=54.3°) (JCPDS card No. 43-1027) diffraction peaks are present in Fig. S1d. With the thermal treatment temperature continuously increasing to 580 °C or 680 °C, the Ni and Ru species mainly appeared with the form of reduced state Ni(0) and Ru(0) owing to the reducing capacity of carbon black at high temperature.

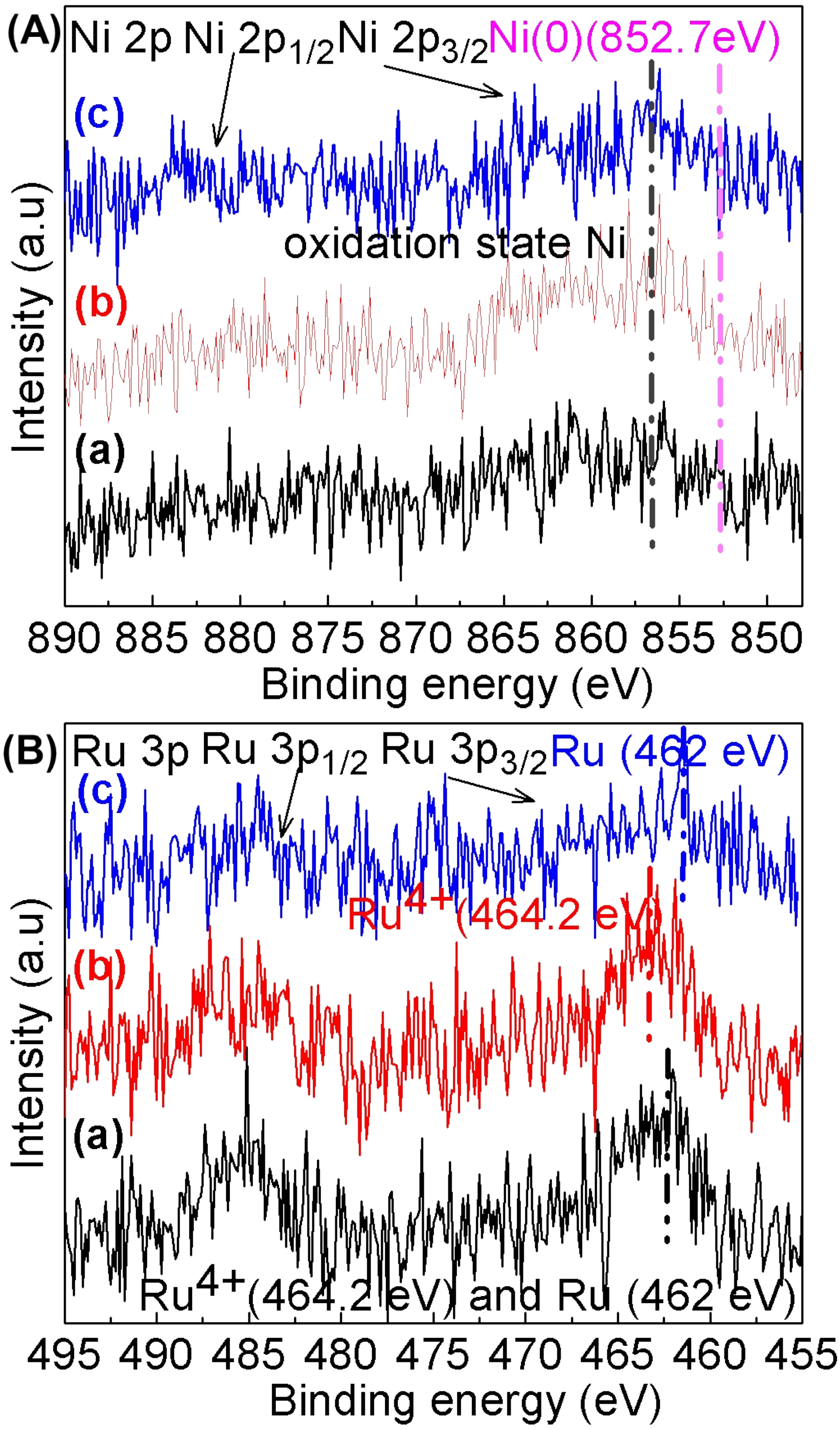


**Fig. S2** (A) Ni 2p XPS and (B) Ru 3p spectra for (a) RuNi/C~380~PVP, (b) RuNi/C~480~PVP and (c) RuNi/C~680~PVP.

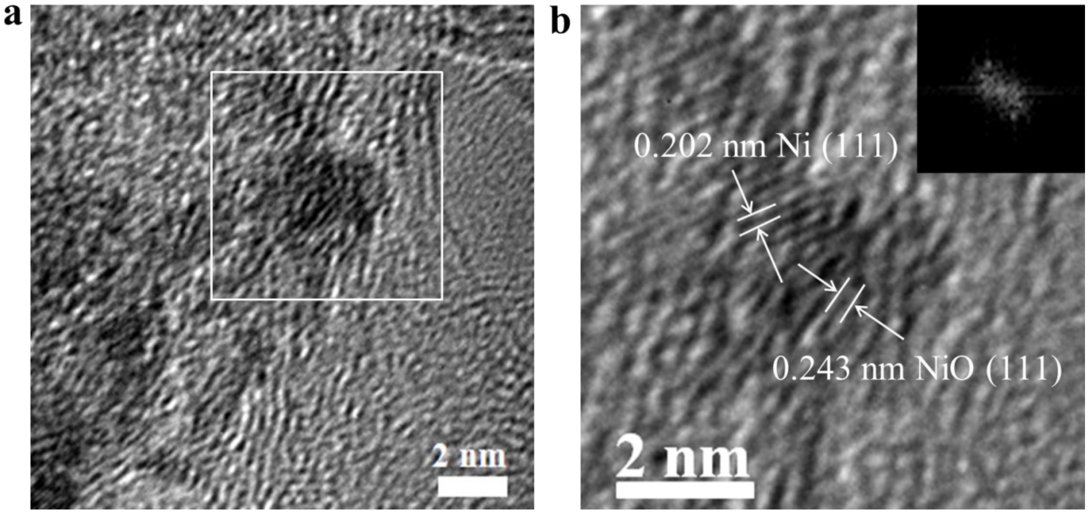


**Fig. S3** (a) HRTEM image for the Ni/NiO/C sample and (b) Enlarged view of the selected area in image a. The indicated lattice fringes, 0.202 nm and 0.243 nm, corresponding to Ni(111) planes (JCPDS card No. 04-0850) and NiO(111) (JCPDS card No. 47-1049), respectively. The inset in (b) shows fast Fourier transform (FFT) patterns results. It indicates that Ni/NiO NPs are small and also with high dispersion.

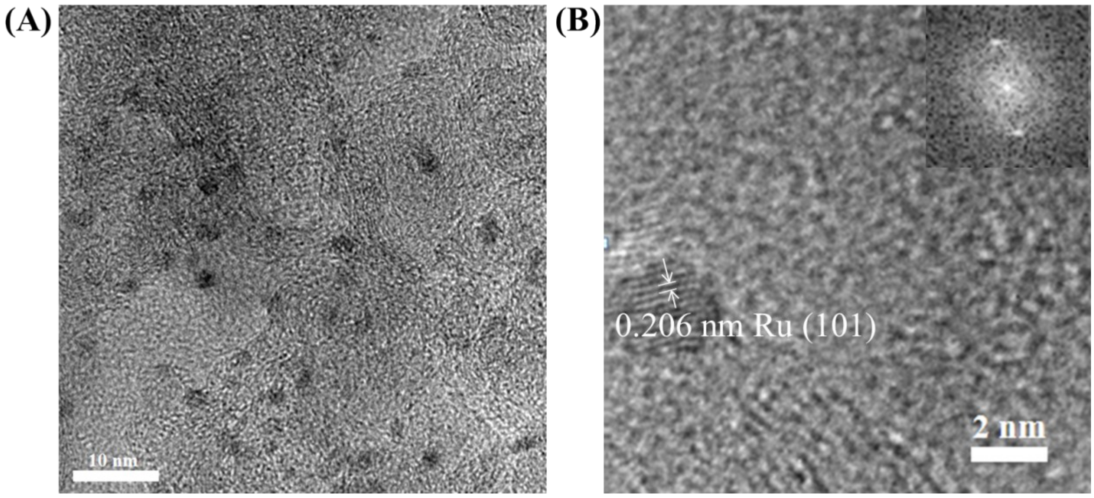


**Fig. S4** (A) TEM and (B) HRTEM images for the 1.25%Ru/C~380~$N_2$+$H_2$ sample. The indicated lattice fringes-0.206 nm corresponds to Ru(101) facets (JCPDS card No. 06-0663). The inset in (b) shows fast Fourier transform (FFT) patterns results. It suggests that Ru NPs are highly dispersed on the support, without any agglomeration.

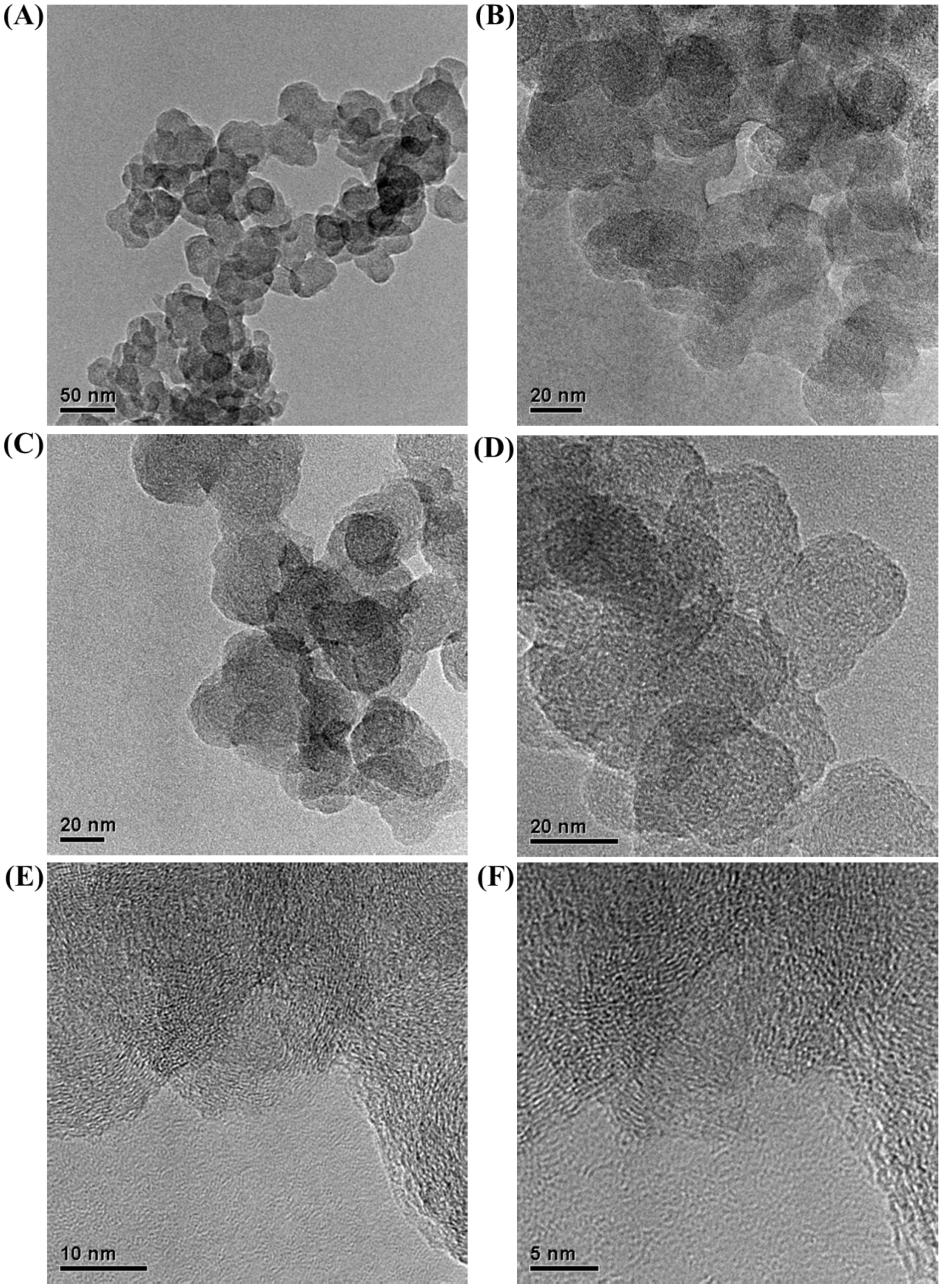


**Fig. S5** (A-D) TEM images for the RuNi/C~uncalcined~PVP sample. (E, F) HRTEM images for the RuNi/C~uncalcined~PVP sample.

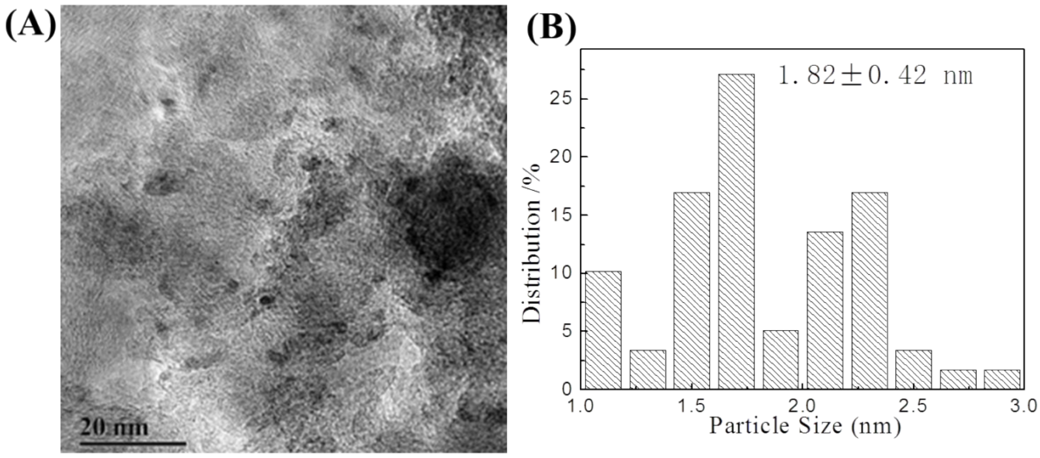


**Fig. S6** (A) TEM image and (B) RuNi BNPs size distribution for the RuNi/C~160 sample. By counting more than 100 RuNi NPs, the size distribution and mean size of RuNi NPs were obtained. The size distribution was very narrow and the average size was about 1.82 nm.

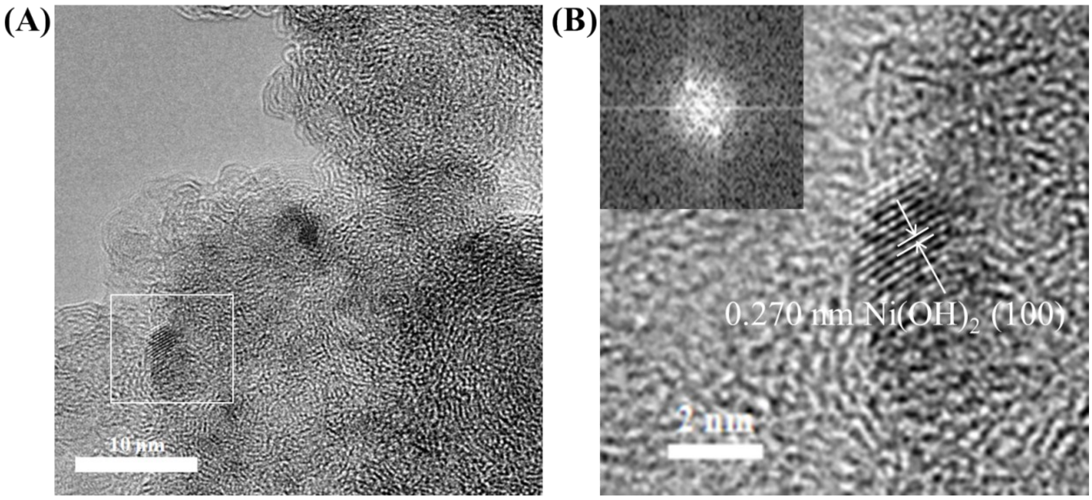


**Fig. S7** (A) HRTEM image for the RuNi/C~160 sample. Scale bar, 10 nm. (B) Enlarged view of the selected area in image A. Scale bar, 2 nm. The indicated lattice fringes, 0.270 nm, corresponding to $Ni(OH)_2$(100) facets (JCPDS card No. 14-0117). The inset in (b) shows fast Fourier transform (FFT) patterns results. It indicates that $Ni(OH)_2$ remained in the sample due to the low annealing temperature (160 °C).

# Notes and references


1 S. Niembro, S. Donnici, A. Shafir, A. Vallribera, M. L. Buil, M. A. Esteruelas and C. Larramona, *New J. Chem.*, 2013, **37**, 278-282.

2 F. Su, L. Lv, F. Y. Lee, T. Liu, A. I. Cooper and X. S. Zhao, *J. Am. Chem. Soc.*, **129**, 2007, 14213-14223.

3 M. Zahmakıran, Y. Tonbul and S. Özkar, *J. Am. Chem. Soc.*, 2010, **132**, 6541-6549.

4 S. Miao, Z. Liu, B. Han, J. Huang, Z. Sun, J. Zhang and T. Jiang, *Angew. Chem. Int. Ed.*, 2006, **45**, 266-269.

5 K. X. Yao, X. Liu, Z. Li, C. C. Li, H. C. Zeng and Y. Han, *ChemCatChem*, 2012, **4**, 1938-1942.

6 Y. Ma, Y. Huang, Y. Cheng, L. Wang and X. Li, *Appl. Catal., A*, 2014, **484**, 154-160.

7 O. Domínguez-Quintero, S. Martínez, Y. Henríquez, L. D'Ornelas, H. Krentzien and J. Osuna, *J. Mol. Catal. A: Chem.*, 2003, **197**, 185-191.

8 Y. Tonbul, M. Zahmakiran and S. Özkar, *Appl. Catal., B*, 2014, **148**, 466-472.

9 J. Schulz, A. Roucoux and H. Patin, *Chem. Eur. J.*, 2000, **6**, 618-624.

10 H. -B. Pan and C. M. Wai, *J. Phys. Chem. C*, 2009, **113**, 19782-19788.

11 P. Barbaro, C. Bianchini, V. Dal Santo, A. Meli, S. Moneti, C. Pirovano, R. Psaro, L. Sordelli and F. Vizza, *Organometallics*, 2008, **27**, 2809-2824.

12 B. Yoon, H. -B. Pan and C. M. Wai, *J. Phys. Chem. C*, 2009, **113**, 1520-1525.

13 H. Duan, D. Wang, Y. Kou and Y. Li, *Chem. Commun.*, 2013, **49**, 303-305.

14 U. G. Hong, J. K. Kim, J. Lee, J. K. Lee, J. H. Song, J. Yi and I. K. Song, *Appl. Catal., A*, 2014, **469**, 466-471.

15 M. Endo, Y. A. Kim, T. Takeda, S. H. Hong, T. Matusita, T. Hayashi and M. S. Dresselhaus, *Carbon*, 2001, **39**, 2003-2010.

16 H. -B. Zhang, G. -D. Lin, Z. -H. Zhou, X. Dong, and T. Chen, *Carbon*, 2002, **40**, 2429-2436.